

Gauge fixing for heat-transport simulations

Aris Marcolongo,^{1,*} Loris Ercole,^{2,2} and Stefano Baroni²

¹*Cognitive Computing and Computational Sciences Department,*

IBM Research – Zürich, Säumerstrasse 4, CH-8803 Rüschlikon, Switzerland

²*SISSA – Scuola Internazionale Superiore di Studi Avanzati, Via Bonomea 265, 34136 Trieste, Italy[†]*

Thermal and other transport coefficients were recently shown to be largely independent of the microscopic representation of the energy (current) densities or, more generally, of the relevant conserved densities/currents. In this paper we show how this *gauge invariance*, which is intimately related to the intrinsic indeterminacy of the energy of individual atoms in interacting systems, can be exploited to optimize the statistical properties of the current time series from which the transport coefficients are evaluated. To this end, we introduce and exploit a variational principle that relies on the metric properties of the conserved currents, treated as elements of an abstract linear space. Different metrics would result in different variational principles. In particular, we show that a recently proposed data-analysis technique based on the theory of transport in multi-component systems can be recovered by a suitable choice of this metric.

Keywords: Transport properties, Molecular dynamics, Thermal conductivity, Statistical analysis of time series, Gauge invariance of transport coefficients
PACS NUMBERS: 05.60.-k 05.45.Tp 66.10.cd

I. INTRODUCTION

The concept of *gauge invariance* of transport coefficients was introduced and explored in recent works on adiabatic heat^{1,2} and charge transport³ in electronic insulators. In its generality, this principle asserts that transport coefficients, such as thermal and electrical conductivities, are largely independent of the detailed form of the local representation of the conserved quantity (energy, charge, mass) being transported: any two such representations resulting in the same integrated value of the conserved quantity, and whose space correlations are short-range, are bound to yield the same transport coefficient. This finding was instrumental in establishing a rigorous and practicable density-functional theory (DFT) of adiabatic heat transport,^{1,4} based on the Green-Kubo (GK) linear-response approach,^{5,6} and more recently spurred new applications based on different definitions of the heat current.^{7,8} On the other hand, the question naturally arises as to how to exploit this *gauge freedom* in order to optimize the statistical properties of the current time series from which transport coefficients are evaluated, and thus minimize the statistical errors affecting the latter.

This work is devoted to the analysis of possible gauges for thermal transport simulations, i.e. different equivalent microscopic definitions of the heat flux, within the GK framework. The GK approach exploits the fluctuation-dissipation principle, which permits to evaluate non-equilibrium transport coefficients by analyzing the fluctuations of the heat flux during equilibrium molecular dynamics (MD) simulations. We note that other frameworks have been successfully applied to evaluate the thermal conductivity based on MD simulations as well, but requiring the direct simulation of non-equilibrium transport processes. We recall here for example the *approach to equilibrium* technique,⁹ based

on a transient, non stationary, process, and the Müller-Plathe method,¹⁰ imposing an external (kinetic) energy flux by swapping particle velocities. These approaches circumvent the problem of definition of an energy density but require simulation sizes large enough to define a local temperature, and may be affected by non-linear effects. Nevertheless, they have been successfully applied in first-principles and classical frameworks.^{11–14} We cite for completeness an other class of techniques to evaluate thermal conductivity which avoids performing any MD simulation. These methods start with a lattice picture and introduce anharmonic effects via the mesoscopic Boltzmann transport equation. We refer the interested reader to a recent review¹⁵ and references therein.

The GK approach to thermal conductivity, developed much before non-equilibrium approaches, is still an area under active research. Efforts to improve the GK framework are dedicated to estimate size and simulation times required for the evaluation of the transport coefficient^{16,17}. Other lines of research aim at developing novel definitions of the energy flux. For example, Ref. 7 introduces a mask function to deal with periodic boundary conditions and an *ad hoc* definition of atomic energies from first principles; Ref. 18 develops a first-principles heat flux where convective components are neglected; Ref. 8 uses an energy-moment perspective based on the Einstein formulation to estimate the thermal conductivity of solids.

The goal of this work is twofold. First, we want to highlight how the presence of spurious signals can hinder the convergence of GK approaches, especially in first-principles calculations of thermal conductivity of molecular systems. Second, we introduce a general variational approach to fix the transport gauge so as to optimize the statistical properties of the estimator of the conductivity, thus reducing simulation times as much as possible. Such an operation reveals to be beneficial in keeping the statistical noise of the conductivities estimated from

first-principles simulations at an acceptable level. We stress that all the methodologies proposed in this work are based on the GK formalism and aim at modifying the heat fluxes used in the GK formulas in a computationally easy but effective way. From all other aspects, the GK formalism remains unchanged.

For most of the work, we focus on heat transport in solids and one-component, possibly molecular, liquids, for which energy is the only relevant conserved quantity. We thus neglect multi-component liquid systems, where the total momenta of individual species should be considered to correctly define the heat current^{4,19,20}. Nevertheless, we will also discuss a theoretical relation between our formalism and the GK formulas derived in a multi-component setting. When dealing with quantum simulations, we further assume the materials to be electronic insulators, thus excluding electrons as heat carriers. Our discussion will be otherwise as general as possible and will include examples from classical as well as *ab initio* molecular dynamics (MD). For the latter, we will follow the GK formulation developed in Ref. 1.

The rest of the work is organized as follows. In Sec. II we introduce our general variational approach and discuss how it can be used to eliminate the ineffective but slowly-decaying signals that may appear in the classical and first-principles simulation of transport coefficients. In Sec. III we present two different implementations of the general variational principle, and Sec. IV is devoted to their comparison. In Sec. V we show how a recently introduced data-analysis technique, based on the theory of multi-component systems,¹⁹ can be derived from the variational principle outlined in the present paper, thus providing novel insight into the known formulas. Finally, Sec. VI contains our conclusions.

II. THEORETICAL BACKGROUND

A. Variational formulation

In one-component isotropic systems the GK equation expresses the thermal conductivity in terms of the time autocorrelation function of the energy flux as:

$$\kappa = \frac{1}{3Vk_B T^2} \int_0^\infty \langle \mathbf{J}(t) \cdot \mathbf{J}(0) \rangle dt, \quad (1)$$

where V is the system's volume, k_B the Boltzmann constant, T the temperature, $\mathbf{J}(t) = \int \mathbf{j}(\mathbf{r}, t) d\mathbf{r}$ is the macroscopic energy current, usually referred to as the *heat* (or energy) *flux*, $\mathbf{j}(\mathbf{r}, t)$ is the energy current density and $\langle \cdot \rangle$ indicates an equilibrium average over molecular trajectories in the microcanonical (NVE) ensemble.^{4-6,21,22} The integral of the autocorrelation function of the energy flux in Eq. (1) can also be interpreted as the zero-frequency component of its power spectrum, and is often called the GK integral. The energy flux $\mathbf{J}(t)$ is a classical observable, *i.e.* a function defined over the phase space of the system: $\mathbf{J}(t) = \mathbf{J}(\Gamma_t)$,

where $\Gamma_t \equiv \{\mathbf{r}_i(t), \mathbf{v}_i(t)\}$ indicates the system's phase-space position at time t and \mathbf{r}_i and \mathbf{v}_i the position and velocity of the i -th atom. The set \mathcal{O} of all such observables is naturally endowed with the structure of a real vector space, via pointwise addition and multiplication.

In order to proceed further, we first define an *inert* or *non-diffusive* flux as one such that its GK integral, Eq. (1), vanishes. Interestingly, adding a non-diffusive energy flux to a diffusive one does not change the value of the conductivity calculated from the latter, an intuitive result that was rigorously proven in Ref. 1 and that is at the basis of the whole concept of gauge invariance of transport coefficients. Nevertheless, non-diffusive terms may increase the power of the noise of the time series to such a level as to compromise its analysis and thus making a numerical estimate of the conductivity too expensive. This suggests one to devise new “optimized” definitions of the energy flux, whereby signal components known to be non-diffusive are conveniently eliminated, thus reducing the power of the noise without affecting the value of the signal.

Let us suppose for the moment that a set of linearly independent such non-diffusive signals $\{\mathbf{Y}_n\}$, $n = 1, \dots, N$ can be identified. Then, the new time series

$$\mathbf{J}' \equiv \mathbf{J} - \sum_n \lambda_n \mathbf{Y}_n, \quad (2)$$

will provide, by replacing \mathbf{J} with \mathbf{J}' into Eq. (1) and with infinite sampling, the same thermal conductivity as the one computed using the original heat flux \mathbf{J} for any choice of the $\{\lambda_n\}$ coefficients. In order to minimize the statistical noise, we should minimize the magnitude of inert signals. To achieve this goal, let us introduce a generic scalar product (\cdot, \cdot) on the vector space \mathcal{O} of observables, inducing a norm $\|A\| \equiv \sqrt{(A, A)}$. For the moment, we leave the scalar product unspecified. We now propose to choose as optimal coefficients those that minimize the function:

$$f(\{\lambda_n\}) \equiv \left\| \mathbf{J} - \sum_n \lambda_n \mathbf{Y}_n \right\|^2, \quad (3)$$

which is the standard loss function used in a multiple-linear regression framework. From a geometrical point of view, the chosen \mathbf{J}' is the component of \mathbf{J} orthogonal to the subspace generated by the non-diffusive signals. We note that, as long as the scalar product is positive definite (*i.e.* $(A, A) > 0$, if $A \neq 0$) and the non-diffusive signals are linearly independent the quadratic form in Eq. (3) is positive definite and has a unique minimum.

Finally, we note also that the variational framework applies directly to the case of anisotropic systems as well. Thermal conductivity becomes then a tensor $\kappa_{\alpha, \beta}$, a function of the cross correlations $\langle J^\alpha(t) J^\beta(0) \rangle$. In this case it is possible to optimize \mathbf{J}' component by component: $J'_\alpha = J_\alpha - \sum_n \lambda_{n, \alpha} Y_{n, \alpha}$, where the $\lambda_{n, \alpha}$ are chosen to minimize $\|J_\alpha - \sum_n \lambda_{n, \alpha} Y_{n, \alpha}\|^2$, for each α under the chosen norm. Evaluating the thermal conductivity tensor

using \mathbf{J}' instead of \mathbf{J} in the tensorial version of Eq. (1) would still lead to the same thermal conductivity thanks to the non-diffusivity of the signals $Y_{n,\alpha}$, but this replacement is expected to reduce the computational cost. For simplicity, in this work we focus on isotropic systems.

B. Inert signals in *ab initio* simulations

The estimate of thermal conductivity from the GK equation, (1), poses serious numerical challenges, especially in *ab initio* MD simulations, where the size and time scales that can be afforded are limited. Even though efficient and automated estimators of κ have been recently devised,¹⁶ non-diffusive components may increase the variance of the energy-flux time series considerably, thus slowing down the convergence of the estimator, as for example it was observed in the case of liquid water¹ or silica glass.²³

One of the most important sources of inert signals that can be identified in *ab initio* simulations is related to the large atomic binding energies affecting the Born-Oppenheimer energies of extended systems. In order to understand what is at stake here, let us consider the case where an all-electron picture of the electronic structure is adopted. Evidently, the nuclei undergoing thermal diffusion drag core electrons around and, with them, the large binding energies rigidly attached to them: these energies are not available to any physical processes accessible at thermal energies and do not contribute therefore to heat transport, while they do increase the magnitude of the energy-flux fluctuations, thus enormously enhancing the noise affecting the estimator of the conductivity. Even in a pseudo-potential picture, cohesion energies are a small fraction of the Born-Oppenheimer total energies, which are therefore dominated by the atomic *binding energies*, $\{\epsilon^S\}$, defined as the energies necessary to remove all the valence electrons from an isolated atom of the S -th species. The energy density associated to such binding energies has the form: $\sum_i \epsilon^{S(i)} \delta(\mathbf{r} - \mathbf{r}_i)$, $S(i)$ being the species of the i -th atom, and \mathbf{r}_i its position.

To fix the notation, in this work capital Latin letters refer to atomic species, and Latin lowercase letters refer to atomic indexes; Greek letters are reserved for Cartesian coordinates, and a summation over repeated Cartesian indexes is implied. We denote with $\mathbf{V}^S = \sum_{\{i \in S\}} \mathbf{v}_i$ the sum of the velocities of all the atoms of species S , which is sometimes called the macroscopic *particle current*. We call \mathbf{W}^S the velocity of the center of mass of the corresponding atomic species: $\mathbf{W}^S = \mathbf{V}^S/N^S$, where N^S is the number of atoms of species S . According to these definitions, the energy current associated to the binding energy reads:

$$\mathbf{J}^{\text{bind}} = \sum_S N^S \epsilon^S \mathbf{W}^S. \quad (4)$$

In a mono-atomic fluid, \mathbf{J}^{bind} is constant because of momentum conservation and it vanishes in the center-of-

mass reference frame; in solids, it is clearly non-zero and non-diffusive, since atoms individually do not diffuse; and in molecular fluids it can be proven that the particle currents are non-diffusive as well.^{1,4,24}

In general, the energy of isolated atoms is not considered in classical, semi-empirical potentials. Nevertheless, the time-averaged atomic energies formally behave as atomic binding energies and they can be safely subtracted from the definition of the atomic energies entering the expression of the energy flux, without altering the value of the resulting heat conductivity; *i.e.* the heat conductivity is invariant with respect to the transformation $\epsilon_i \rightarrow \epsilon_i - \bar{\epsilon}^{S(i)}$, where $\bar{\epsilon}^S$ is the average energy of atoms of species S . In general, classical mean atomic energies are much smaller than the typical atomic binding energies in first-principles simulations, thus leading to smaller inert fluxes.

III. TECHNIQUES

The most common choice of scalar product between two real observables $A, B \in \mathcal{O}$ is given by the static cross-correlation, which we refer to as the *microcanonical (MC) scalar product*:

$$(A, B)_{\text{MC}} \equiv \langle AB \rangle = \int P_{\text{NVE}}(\Gamma) A(\Gamma) B(\Gamma) d\Gamma, \quad (5)$$

where P_{NVE} is the constant energy distribution of the microcanonical ensemble, explored ergodically via Hamiltonian dynamics. For vector observables, the product AB implies a scalar product as well. The last expression makes it clear that the MC scalar product is positive definite. In this section we explore different optimization techniques based on this choice of the metric in Eq. (2) and (3).

The minimization of Eq. (3), *i.e.* the projection onto the subspace orthogonal to the inert fluxes, can be directly performed by differentiating Eq. (3) with respect to λ_m and obtaining the linear system:

$$\langle \mathbf{J} \cdot \mathbf{Y}_n \rangle - \sum_m \lambda_m \langle \mathbf{Y}_m \cdot \mathbf{Y}_n \rangle = 0, \quad n = 1, \dots, N. \quad (6)$$

The thermal conductivity can be then computed via the GK equation (1), by replacing \mathbf{J} with \mathbf{J}' , that is defined in Eq. (2) using the $\{\lambda_n\}$ coefficients that solve Eq. (6). This technique has been instrumental in computing the heat conductivity of liquid water from an energy-flux time series that would have been otherwise affected by an intractable numerical noise.¹ We note that the new energy current \mathbf{J}' is computed from the difference of the original current and the weighted inert fluxes, *i.e.* a difference of signals of large amplitude. We refer to this procedure as the *decorrelation technique*, since the solution of Eq. (6) is equivalent to imposing that the current \mathbf{J}' is decorrelated with respect to each inert signal $\{\mathbf{Y}_n\}$.

We now discuss how, when the \mathbf{Y} currents are assumed to coincide with the average velocities of the various

atomic species, $\{\mathbf{Y}_n\} = \{\mathbf{V}^S\}$, decorrelation is equivalent to a different *renormalization* procedure of the individual atomic velocities. Velocity renormalization does not require the solution of any linear system and involves only operations with small-amplitude signals. Let $\mathbf{J}_{\text{bare}}(\{\mathbf{r}_i, \mathbf{v}_i\})$ be the heat current, a function of the atomic coordinates $\{\mathbf{r}_i, \mathbf{v}_i\}$. The renormalized heat current is defined as:

$$\mathbf{J}_{\text{ren}}(\{\mathbf{r}_i, \mathbf{v}_i\}) \equiv \mathbf{J}_{\text{bare}}(\{\mathbf{r}_i, \mathbf{v}_i - \mathbf{W}^{S(i)}\}), \quad (7)$$

where in the renormalized velocities $\mathbf{v}'_i \equiv \mathbf{v}_i - \mathbf{W}^{S(i)}$ the velocity of the centre of mass of the respective species has been subtracted. The renormalized current can be computed without any coding effort by any program providing an energy current by replacing input velocities with their renormalized values and leaving the positions unchanged. The non diffusive particle current \mathbf{V}^S has been effectively set to zero in the definition of \mathbf{J}_{ren} .

We demonstrate the effectiveness of the renormalization procedure by performing several classical MD simulations of liquid water at ambient conditions, adding a fictitious formation energy term to each species and studying the effects on the resulting energy currents. Simulations were carried out using the LAMMPS molecular dynamics code,²⁵ at ambient conditions, in a cubic box containing 216 water molecules, considering a flexible model of water²⁶ and an integration time step of 0.5 fs (further simulation details are reported in Appendix D). A species-dependent shift was added to the instantaneous atomic energies: $\epsilon_i \rightarrow \epsilon_i + \bar{\epsilon}^{S(i)}$. We chose small values for the formation energies: $\bar{\epsilon}^H \approx -0.2, -0.4$ eV, and $\bar{\epsilon}^O \approx -0.4, -0.9$ eV, *i.e.* values that are higher than the typical interaction energies but much lower than the formation energies considered in DFT. Even such a small perturbation can have an impact on the convergence properties of the GK current. In Fig. 1(a) we plot the thermal conductivity estimated by a direct integration of the energy-flux autocorrelation function, Eq. (1), as a function of the upper integration limit (see Appendix D for a numerical expression), using the original definition of the energy current ($\mathbf{J}_{\text{bare}}^{\{0,0\}}$), several definitions with additional formation energies ($\mathbf{J}_{\text{bare}}^{\{\bar{\epsilon}^H, \bar{\epsilon}^O\}}$), and the latter after renormalization was applied (\mathbf{J}_{ren}). The addition of formation energies increases the variance of the time series and slows down the convergence of the GK integral, thus requiring one to run longer simulations in order to converge the integral with similar accuracy. Nevertheless, as expected, all the integrals converge to the same value after a sufficient integration time. Once the renormalization procedure is performed, the convergence becomes much faster and the integral resembles to the one computed from $\mathbf{J}_{\text{bare}}^{\{0,0\}}$. Notice that renormalizing any of the time series returns exactly the same \mathbf{J}_{ren} . Additional information can be inferred from the power spectrum of the energy current, defined as $S(\omega) = \frac{1}{T} \left\langle \left| \int_0^T \mathbf{J}(t) e^{i\omega t} dt \right|^2 \right\rangle$ and plotted in Fig. 1(b), which clearly shows that forma-

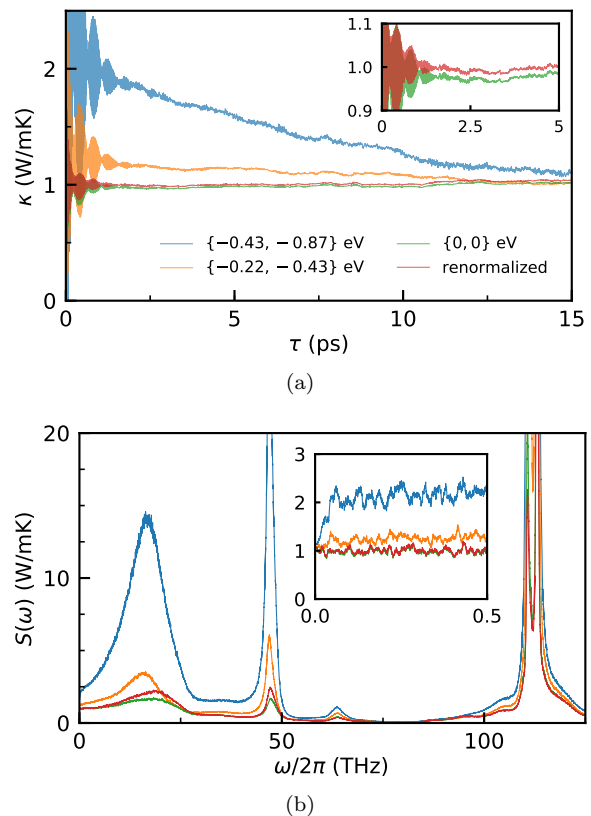


FIG. 1. Convergence behavior of the thermal conductivity obtained from different definitions of the energy current of classical liquid water. Species-dependent formation energies $\{\bar{\epsilon}^H, \bar{\epsilon}^O\}$ were added (see legend and text). In particular, the red line represents the renormalized current. (a) Thermal conductivity computed from the GK equation, Eq. (1), as a function of the upper integration limit (see Appendix D for a numerical definition). Inset: zoom of the low- τ region. (b) Power spectrum of the energy current, whose zero-frequency value is the thermal conductivity. Inset: zoom of the low-frequency region.

tion energies lead to an increase in the power of the signal (the integral of the spectrum). The zero-frequency value of the spectrum, which is proportional to the thermal conductivity,^{4,16} is not affected by the definition used, but becomes more and more difficult to estimate when larger formation energies are considered, due to the fast increase of $S(\omega)$ at $\omega \sim 0$.

We now repeat the same kind of analysis in an *ab initio* framework considering amorphous silica, a-SiO₂, a multi-component solid, at ~ 350 K. For reference, in Appendix D we report the formulas used to evaluate the bare first-principles energy current. For the purpose of this calculation and to save computational time we considered a small cell of 72 atoms, we generated the trajectory via the classical BKS interatomic potential²⁷, and for 10000 snapshots (corresponding to 100 ps of trajectory) we computed the energy current using the classical and *ab initio* definitions (further simulation details in Appendix D). Finally, we applied the renormaliza-

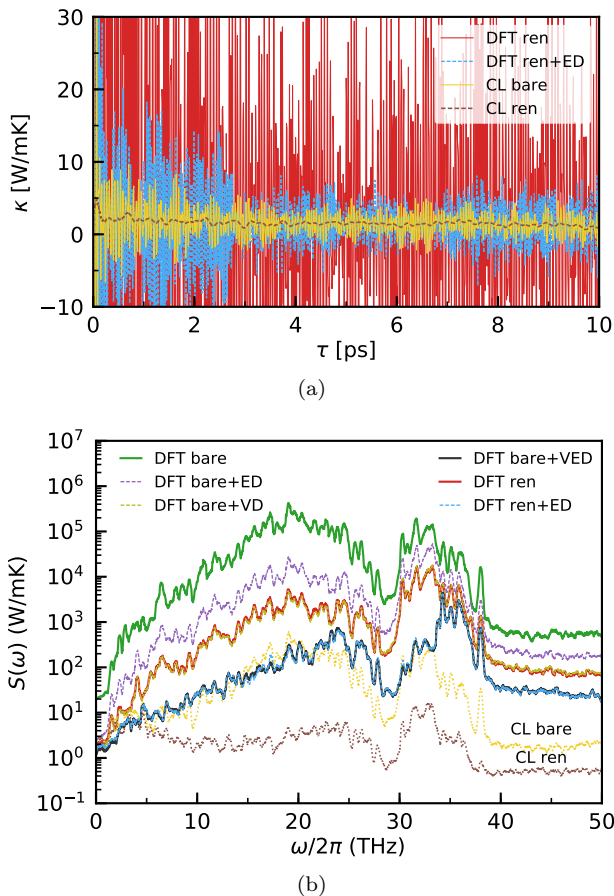


FIG. 2. Analysis of different definitions of the energy current of a 72-atom sample of a-SiO₂. The original \mathbf{J}_{bare} classical (CL) and DFT definitions have been renormalized, obtaining \mathbf{J}_{ren} . Also reported are the same currents decorrelated with respect to the particle current of one species (VD), the electronic current (ED), or both (VED). (a) Thermal conductivity computed from the GK equation, Eq. (1), as a function of the upper integration limit. The result of the bare DFT current is out of scale and has been omitted. (b) Power spectrum of the energy currents. The zero frequency corresponds to κ .

tion procedure to the latter. Let us remark that in order to compute κ from first principles one should generate the trajectory by *ab initio* MD, nevertheless we use this expedient to observe the effects of the different energy-current definitions, without including the effects of the different dynamics. For the DFT calculations we used the QUANTUM ESPRESSO package²⁸ with a PBE functional²⁹, a plane-wave cutoff of 80 Ry, and optimized norm-conserving Vanderbilt pseudopotentials (ONCVP)³⁰. In Fig. 2(a) we plot the GK integrals, which feature very large oscillations, making a direct estimate of κ extremely difficult. In particular, the integral of the DFT bare energy current $\mathbf{J}_{\text{bare}}^{\text{DFT}}$ is out of scale and is not shown. Much more information can be gained from the power spectra of the currents, reported in Fig. 2(b) on a logarithmic scale. We immediately notice the much larger power of the $\mathbf{J}_{\text{bare}}^{\text{DFT}}$ time series (labeled

\mathbf{J} definition	a-SiO ₂	H ₂ O
DFT bare	25.5 ± 5.9	740 ± 140
DFT ren	1.31 ± 0.29	1.18 ± 0.17
Classic bare	1.32 ± 0.29	–
Classic ren	1.28 ± 0.26	–
DFT bare, VD	1.30 ± 0.28	0.99 ± 0.15
DFT bare, ED	2.79 ± 0.61	341 ± 46
DFT bare, VED	0.95 ± 0.21	0.82 ± 0.12
DFT ren, ED	1.11 ± 0.24	1.03 ± 0.15

TABLE I. Thermal conductivities (W/mK) estimated via cepstral analysis from different definitions of the energy current (parameters used in the analysis are reported in Appendix D). VD, ED, and VED indicate a current that has been decorrelated with respect to the particle current of a species \mathbf{V}^S , the electronic current \mathbf{J}_{el} , or both, respectively. Errors are one standard deviation.

“DFT bare”, top left) with respect to the classical one (labeled “CL bare”, bottom right). Indeed, the standard deviation of $\mathbf{J}_{\text{bare}}^{\text{DFT}}$ (proportional to the integral of the spectrum) is 25 times larger than the classical one $\mathbf{J}_{\text{bare}}^{\text{cl}}$, and in both cases the renormalization reduces the standard deviations of the currents by a factor of ≈ 5 . The huge power of the bare DFT current makes an estimate of κ impossible to converge to physical values with the trajectory lengths attainable with *ab initio* MD. Renormalization allows one to solve this problem and to obtain meaningful results, which are also compatible with the classical values, as reported in Table I in the fields “DFT ren”, “Classic bare”, and “Classic ren”. Although these simulations were not meant to obtain quantitatively accurate values, the thermal conductivities are in fairly good agreement with previous experiments and computational studies ($\kappa_{\text{exp}} \approx 1.4$ W/mK)³¹. More reliable and accurate results would require a more careful choice of the force field and a study of the system-size dependence of κ , which is especially critical in the case of amorphous systems.²³

It is possible to prove formally the equivalence of the transport coefficients computed from the bare and renormalized currents, $\kappa_{\text{bare}} = \kappa_{\text{ren}}$, starting with the following generic expression of a component of a GK energy flux:

$$J_{\text{bare},\alpha} = \sum_i \left(\frac{1}{2} m_i v_i^2 \right) v_{i,\alpha} + \sum_i \varepsilon_{\alpha\beta}^i(\{\mathbf{r}\}) v_{i,\beta}. \quad (8)$$

Any atomic energy current, defined as the time derivative of the first moment of an energy density, can be reduced to such a form, the matrices $\varepsilon_{\alpha\beta}^i$ being functions of coordinates only (dependent on the local environment) and not of particle velocities. From Eq. (7) and after some manipulations, the renormalized current can be related to the bare one:

$$J_{\text{ren},\alpha} = J_{\text{bare},\alpha} - \sum_S h_{\alpha\beta}^S V_\beta^S + J'_\alpha, \quad (9)$$

where the precise forms of the time-independent h -matrices and the residual current \mathbf{J}' are provided in Ap-

pendix A. Adding a non-diffusive signal does not change the transport coefficient: the desired result will thus follow from the non-diffusivity of the signal $\Delta \mathbf{J} = \mathbf{J}_{\text{bare}} - \mathbf{J}_{\text{ren}} = \sum_S h^S \mathbf{V}^S - \mathbf{J}'$. In Appendix A we show that the residual current \mathbf{J}' can be neglected in the thermodynamic (TD) limit, leading to the relation:

$$\frac{1}{V} \langle \Delta \mathbf{J}(t) \cdot \Delta \mathbf{J}(0) \rangle dt \sim \sum_{S,S'} h_{\alpha\beta}^S h_{\alpha\beta'}^{S'} \frac{\langle V_{\beta}^S(t) V_{\beta'}^{S'}(0) \rangle}{V}. \quad (10)$$

The expectation value $\frac{1}{V} \langle V_{\beta}^S(t) V_{\beta'}^{S'}(0) \rangle \sim \mathcal{O}(1)$, thus bringing a non-vanishing contribution in the TD limit. However, as already observed, in solids, amorphous materials and one-component molecular liquids the signals V_{β}^S are non-diffusive and therefore every cross-correlation $\langle V_{\beta}^S(t) V_{\beta'}^{S'}(0) \rangle$ has a vanishing zero-frequency component, as a consequence of the lemma in Ref. 1. Therefore, even if the signal $\Delta \mathbf{J}$ in general shows a non-zero auto-correlation function, its integral from zero to infinity has a vanishing value in the TD limit.

IV. RELATION BETWEEN DECORRELATION AND RENORMALIZATION

The two methodologies are related by the fact, proven in Appendix B, that in the TD limit the coefficients h of Eq. (9) solve the same linear system that was derived by the decorrelation criterion, Eq. (6), with $\{\mathbf{Y}_n\} = \{\mathbf{V}^S\}$. According to Eq. (9), since in the TD limit the residual current can be neglected, one has that $\mathbf{J}_{\text{ren}} \sim \mathbf{J}_{\text{bare}} - \sum_S h^S \mathbf{V}^S$ and therefore the decorrelation becomes equivalent to the energy-flux renormalization. This result poses an application of both methods on solids grounds. The decorrelation technique, however, can also be performed with respect to other types of non-diffusive signals, such as the adiabatic electronic current \mathbf{J}_{el} (defined in Appendix E).

We compare numerically the two techniques using the *ab initio* energy currents of a-SiO₂ and reporting all the estimated thermal conductivities in Table I. These values and their statistical errors have been obtained using the cepstral analysis technique, which exploits the statistical properties of the power spectrum of the energy current, $S(\omega)$, to estimate the thermal conductivity in an efficient and straightforward way.^{16,32} The parameters used in the analysis are reported in Appendix D. As we previously noted, the bare current $\mathbf{J}_{\text{bare}}^{\text{DFT}}$ leads to an overestimation of κ (field “DFT bare” in the table) that can be corrected by applying the renormalization procedure (“DFT ren”). Equivalently, one could decorrelate $\mathbf{J}_{\text{bare}}^{\text{DFT}}$ from one particle current³³, *i.e.* \mathbf{V}^{Si} or \mathbf{V}^{O} , thus obtaining a signal that gives a κ compatible with the one obtained from $\mathbf{J}_{\text{ren}}^{\text{DFT}}$ (“DFT bare, VD”). We also notice that the power spectra of these two signals are almost identical (labeled “DFT bare + VD” and “DFT ren” in Fig. 2(b)), confirming the equivalence of the decorrelation and renormalization methods. As one may suspect,

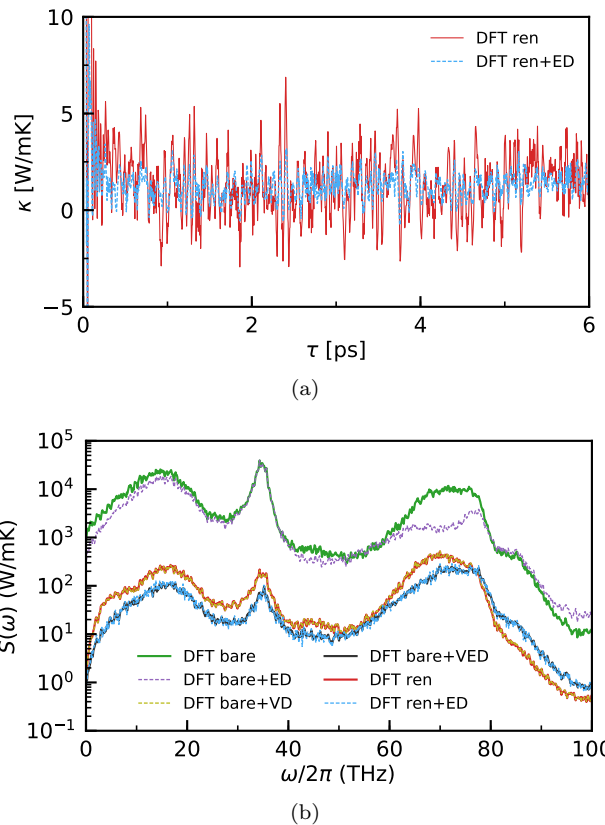


FIG. 3. Analysis of different definitions of the energy current of *ab initio* water. The original \mathbf{J}_{bare} DFT definition has been renormalized, obtaining \mathbf{J}_{ren} . Also reported are the same currents decorrelated with respect to the particle current of one species (VD), the electronic current (ED), or both (VED). (a) Thermal conductivity computed from the GK equation, Eq. (1), as a function of the upper integration limit. The result of the bare DFT current is out of scale and has been omitted. (b) Power spectrum of the energy currents. The zero frequency corresponds to κ .

decorrelation with respect to the particle velocities has no effect when applied to \mathbf{J}_{ren} , in which the sum of all the renormalized velocities is zero by construction (see Appendix B, Eq. (B3) for a formal justification).

Moreover, one can try to decorrelate the current from other non-diffusive signals, in order to further decrease the power of the noise. For example, if we decorrelate $\mathbf{J}_{\text{bare,VD}}^{\text{DFT}}$ or $\mathbf{J}_{\text{ren}}^{\text{DFT}}$ from the electronic current \mathbf{J}_{el} (see definition in Appendix E), we obtain a signal whose power is reduced by an additional factor of ≈ 3 , and that gives a compatible thermal conductivity (fields “DFT bare, VED” and “DFT ren, ED”, respectively).

However, the particle current appears to be the largest source of inert signals in this system. In fact, if we were to decorrelate the bare current $\mathbf{J}_{\text{bare}}^{\text{DFT}}$ solely with respect to \mathbf{J}_{el} , we would not obtain a correct value of κ (“DFT bare, ED”), because the power of the spectrum would still be too large (*i.e.* just a factor ≈ 3 smaller than the power of $\mathbf{J}_{\text{bare}}^{\text{DFT}}$), thus compromising its analysis.

Finally, we performed the same analysis on *ab initio* heavy water at ambient conditions. The simulation was performed with the same setting of Ref. 1. Similarly to silica, an analysis of the bare current $\mathbf{J}_{\text{bare}}^{\text{DFT}}$ returns an unphysical value of κ , reported in Table I. The renormalization procedure or the decorrelation with respect to a particle signal should be applied in order to obtain a physical value of κ , which is compatible with the one originally estimated by Marcolongo *et al.*¹ Moreover, a decorrelation with respect to the electronic current \mathbf{J}_{el} can also be applied and gives compatible results. The GK integrals and the power spectra of the energy current for the different definitions are displayed in Fig. 3. Ultimately, when dealing with DFT energy currents of solids or one-component liquids, the most effective and efficient strategy proved to be a velocity-renormalization of the energy-current time series followed by a decorrelation with respect to the electronic current. Alternatively, one may obtain similar results by considering the multi-component formalism.

V. RELATION WITH THE MULTI-COMPONENT FORMALISM

The variational framework presented in this work can be exploited to rederive, in an alternative way, the formulas used to evaluate the thermal conductivity of multi-component systems. Here we recall the basic result, following the presentation of Ref. 19. We consider a multi-component system characterized by M linearly independent, conserved fluxes \mathbf{J}_i , $i = 0, \dots, M-1$, individually diffusive and where \mathbf{J}_0 is the energy flux. We then define the matrix:

$$\Lambda_{ij} \equiv \frac{1}{2} \int_{-\infty}^{\infty} \langle \mathbf{J}_i(t) \mathbf{J}_j(0) \rangle dt, \quad i, j = 0, \dots, M-1. \quad (11)$$

The thermal conductivity coefficient in the multi-component setting is then given by:

$$\kappa = \frac{1}{3V k_B T^2} \frac{1}{[\Lambda^{-1}]_{00}}. \quad (12)$$

We shall show that, by taking $\mathbf{Y} = \{\mathbf{J}_i\}_{i=1, \dots, M-1}$ in Eq. (3) and applying our variational framework we can recover the formula of the multi-component theory. In particular, we first start with the bare energy flux \mathbf{J}_0 and decorrelate it with respect to the other conserved fluxes using an *ad-hoc* engineered scalar product. We then evaluate the thermal conductivity by inserting the decorrelated \mathbf{J}'_0 into the single-component GK equation (1). In this way we will recover Eq. (12), showing that the multi-component formula follows by dynamically decoupling the energy current from the other conserved fluxes. Let us use in Eq. (3) the following *Green-Kubo scalar product* between two generic fluxes, A and B :

$$(A, B)_{\text{GK}, \omega} \equiv \frac{1}{2} \int_{-\infty}^{\infty} \langle A(t) B(0) \rangle e^{i\omega t} dt, \quad (13)$$

which is symmetric, bilinear and real. As before, for vector observables like heat fluxes, the product AB implies a scalar product as well. The symmetry property follows from the identity $\langle A(t) B(0) \rangle = \langle B(t) A(0) \rangle$, while the scalar product is real because $\langle A(-t) B(0) \rangle = \langle A(t) B(0) \rangle$. Both identities follow from Onsager's principle of microscopic reversibility³⁴ and reminding that fluxes are odd under time reversal. $(A, B)_{\text{GK}, \omega}$ is also known as the cross-power spectrum, and $(A, A)_{\text{GK}, \omega}$ is the power spectrum of A , which is always ≥ 0 for stationary signals. We note that the GK scalar product is well defined on the subspace generated by a set of signals that are odd under time reversal, and it depends parametrically on the chosen frequency ω . For small $\omega \neq 0$ we can assume the scalar product to be positive definite, whereas any non-diffusive signal has zero norm at $\omega = 0$. Later we will discuss the limit $\omega \rightarrow 0$.

Let us define the (frequency-dependent) matrices:

$$\Lambda_{ij}(\omega) \equiv (\mathbf{J}_i, \mathbf{J}_j)_{\text{GK}, \omega}, \quad i, j = 0, \dots, M-1, \quad (14)$$

$$\Sigma_{ij}(\omega) \equiv \Lambda_{i,j}, \quad i, j = 1, \dots, M-1, \quad (15)$$

$$K_i(\omega) \equiv \Lambda_{i,0} = \Lambda_{0,i}, \quad i = 1, \dots, M-1, \quad (16)$$

where Λ and Σ are symmetric and K is a column vector. We now define: $\mathbf{J}'_0(\omega) = \mathbf{J}_0 - \sum_{i=1}^{M-1} \lambda_i(\omega) \mathbf{J}_i$. For each ω , the vector of coefficients $\{\lambda_i(\omega)\}_{i=1, \dots, M-1}$ that minimizes Eq. (3) (*i.e.* the power spectrum $\|\mathbf{J}'_0(\omega)\|_{\text{GK}, \omega}^2$) is then obtained by decorrelating the energy flux \mathbf{J}_0 with respect to the other particle fluxes and solving the linear system: $\lambda(\omega) = \Sigma(\omega)^{-1} K(\omega)$. If we apply the (frequency-dependent) GK formula, Eq. (1), to the optimized energy flux $\mathbf{J}'_0(\omega)$, we obtain:

$$\kappa(\omega) = \frac{1}{3V k_B T^2} \|\mathbf{J}'_0(\omega)\|_{\text{GK}, \omega}^2 \quad (17)$$

An explicit computation leads to:

$$\begin{aligned} \kappa(\omega) &= \frac{1}{3V k_B T^2} (\Lambda(\omega)_{00} - K(\omega)^\top \Sigma(\omega)^{-1} K(\omega)) \\ &= \frac{1}{3V k_B T^2} \frac{1}{[\Lambda(\omega)^{-1}]_{00}}, \end{aligned} \quad (18)$$

where the last equality follows from writing the inverse of the Λ matrix in a block form¹⁹. Interestingly, in the $\omega \rightarrow 0$ limit Eq. (18) becomes exactly the expression of the thermal conductivity for multi-component systems, which is usually derived from the Onsager relations by imposing the vanishing of all the mass fluxes^{4,19}. The matrix $\Lambda_{ij}(\omega = 0) = (\mathbf{J}_i, \mathbf{J}_j)_{\text{GK}, \omega=0}$ can be assumed to be invertible in this multi-component setting. Furthermore, $\kappa(\omega)$ is proportional to the so-called reduced spectrum, which was defined in Ref. 19 and will always be lower than the power spectrum of both the original and the decorrelated signal, due to the present variational derivation.

In Ref. 19 the formulas of the multi-component formalism were also applied as a tool to remove spurious signals

in polyatomic liquids, by considering the energy flux \mathbf{J}_0 and a generic set of inert signals $\{\mathbf{J}_i\}_{i=1,\dots,M-1}$. Inert signals are non-diffusive by definition, in contrast to the fluxes $\{\mathbf{J}_i\}_{i=1,\dots,M-1}$ considered in the multi-component case. As a consequence, in this case the only non-zero element of $\Lambda(\omega = 0)$ is $\Lambda(\omega = 0)_{00} = (\mathbf{J}_0, \mathbf{J}_0)_{\text{GK}, \omega=0}$ and the matrix is obviously non-invertible. Nevertheless, the limit $\omega \rightarrow 0$ can be taken after the matrix inversion, leading to a well defined scheme. The cepstral analysis technique described in Ref. 19 provides a statistically correct way to obtain the $\omega \rightarrow 0$ limit after the matrix inversion.

VI. CONCLUSIONS

In this work we presented a general framework, based on a variational principle, able to optimize a generic energy-flux time series by removing inert signals that do not contribute to the thermal conductivity. Our method is general and it can be generalized to the computation of other transport coefficients as well, whenever a non-diffusive signal can be identified. In the case of thermal transport, we highlighted why atomic binding contributions can pose serious convergence problems to Green-Kubo thermal conductivity simulations, especially in *ab initio* frameworks and in polyatomic systems. We investigated numerically two solutions to this problem, that use the static cross-correlation as a scalar product between observables in our general framework. The first approach is based on the concept of decorrelation of the energy-current time series, and the second on renormalization of velocities. In the thermodynamic limit the two procedures are shown to be equivalent both from a theoretical and numerical point of view, when the decorrelation technique is used with the particle currents. The decorrelation technique can indeed be applied when a generic slowly-decaying signal makes a direct application of the GK formulas impossible or extremely expensive. The renormalization technique, instead, decorrelates the energy flux with respect to the particle current, but it is more straightforward to apply and can be used to detect whether binding energy contributions are correctly handled. As we demonstrated numerically, ignoring binding energy contributions can lead to wrong results, which cannot be detected by any standard statistical analysis of the heat currents. We therefore propose that both procedures should be performed to ensure that the simulation is not affected by convergence problems due to slowly-decaying signals. In our first-principles calculations we followed the heat-current definition of Ref. 1, but other definitions can be affected by the same problems described in this work, when applied to polyatomic systems.

Finally, we proved formally the equivalence between our general framework and the GK theory of heat transport in multi-component systems, by identifying a scalar product that formalizes the dynamical decoupling be-

tween the fluxes that are associated to the different transport mechanisms in such systems. We think that this work will help to interpret and analyze future applications of the GK theory to the computation of thermal conductivity, both using DFT or advanced force fields.

VII. ACKNOWLEDGMENTS

LE and SB would like to thank Federico Grasselli for many valuable discussions. This work was partially funded by the EU through the MAX Centre of Excellence for supercomputing applications (Project No. 676598).

The authors declare no competing financial interests.

Appendix A: General relation between bare and renormalized currents

We prove here Eq. (9) of the main text, showing the explicit form of the h -matrices and of \mathbf{J}' . We start from Eq. (8) and denote with the an arrow $\xrightarrow{\text{ren}}$ the substitution of velocities with their renormalized values. We also introduce a convenient linear operator δ , acting on a phase-space observable X as $\delta X \equiv X - \langle X \rangle$, which isolates the fluctuations.

Under renormalization, the term linear with the velocities transforms in the following way:

$$\sum_i \epsilon_{\alpha\beta}^i(\{\mathbf{r}\}) v_{i,\beta} \xrightarrow{\text{ren}} \sum_i \epsilon_{\alpha\beta}^i(\{\mathbf{r}\}) v_{i,\beta} - \sum_S \left[\langle \epsilon_{\alpha\beta}^S \rangle + \frac{1}{N_S} \sum_{i \in S} \delta \epsilon_{\alpha\beta}^i \right] V_\beta^S, \quad (\text{A1})$$

where, with a slight abuse of notation, we called $\langle \epsilon_{\alpha,\beta}^S \rangle$ the ensemble mean of $\langle \epsilon_{\alpha,\beta}^i \rangle$ over all atoms of species S , supposed to be equivalent. The kinetic term instead transforms like this:

$$\sum_i \left(\frac{1}{2} m_i v_i^2 \right) v_{i,\alpha} \xrightarrow{\text{ren}} \sum_i \left(\frac{1}{2} m_i v_i^2 \right) v_{i,\alpha} - \sum_S \left[\left(\sum_{i \in S} \frac{1}{2} m_i v_i^2 \right) \frac{V_\alpha^S}{N_S} - m_S \left(\sum_{i \in S} v_{i,\alpha} v_{i,\beta} \right) \frac{V_\beta^S}{N_S} + m_S V_\alpha^S \frac{(V^S)^2}{N_S^2} \right] \quad (\text{A2})$$

The mean values are determined by the equipartition theorem, as:

$$\frac{1}{2} m_i v_i^2 = \frac{3}{2} k_B T + \frac{1}{2} m_i \delta(v_i^2), \quad (\text{A3})$$

$$v_{i,\alpha} v_{i,\beta} = \frac{k_B T}{m_A} \delta_{\alpha\beta} + \delta(v_{i,\alpha} v_{i,\beta}), \quad (\text{A4})$$

thus leading to the following substitutions in Eq. (A2):

$$-\sum_S \left(\sum_{i \in S} \frac{1}{2} m_i v_i^2 \right) \frac{V_\alpha^S}{N_S} = -\sum_S \left[\frac{3}{2} k_B T + \frac{1}{2} m_S \frac{1}{N_S} \sum_{i \in S} \delta(v_i^2) \right] V_\alpha^S, \quad (\text{A5})$$

and

$$-\sum_S m_S \left(\sum_{i \in S} v_{i,\alpha} v_{i,\beta} \right) \frac{V_\beta^S}{N_S} = -\sum_S \left[k_B T \delta_{\alpha,\beta} + m_S \frac{1}{N_S} \sum_{i \in S} \delta(v_{i,\alpha} v_{i,\beta}) \right] V_\beta^S. \quad (\text{A6})$$

Combining Eqs. (A1), (A2), (A5), and (A6) we finally derive Eq. (9) by defining the following h -matrices:

$$h_{\alpha\beta}^S = \langle \varepsilon_{\alpha\beta}^S \rangle + \frac{5}{2} k_B T \delta_{\alpha\beta}. \quad (\text{A7})$$

The residual current \mathbf{J}' has the following form:

$$J'_\alpha = -\sum_S \left[\left(\frac{1}{N_S} \sum_{i \in S} \delta \varepsilon_{\alpha\beta}^i \right) + m_S \left(\frac{1}{N_S} \sum_{i \in S} \delta(v_{i,\alpha} v_{i,\beta}) \right) \right] V_\beta^S. \quad (\text{A8})$$

$$+ \frac{1}{2} m_S \left(\frac{1}{N_S} \sum_{i \in S} \delta(v_i^2) \right) \delta_{\alpha\beta} - m_S \frac{(V^S)^2}{N_S^2} \delta_{\alpha\beta} \Big] V_\beta^S. \quad (\text{A9})$$

We now step back for a moment to define an E -signal as an observable which can be written as a sum of fluctuations δf , $E = \sum_i \delta f(\mathbf{r}_i, \mathbf{v}_i)$, *i.e.* an extensive variable which can be written as a sum of local variables with zero mean. The precise form of the function f depends on the particular E -signal and the sum over i may be restricted to a certain atomic species. One can easily analyze the TD scaling of the autocorrelation functions formed by a finite product of E -signals. Expanding the summations and noticing that fluctuations among particles at large distances are uncorrelated the following result can be obtained:

$$\langle E_1 \cdots E_n \rangle \sim \mathcal{O}(N^{\lfloor n/2 \rfloor}), \quad n \geq 2, \quad (\text{A10})$$

where $\lfloor \cdot \rfloor$ is the floor function.

The residual current in Eq. (A9) has been written explicitly as a finite sum of contributions, each one given by a product of E -signals: $(E_1 \times \cdots \times E_p)/N_S^q$, with $(p, q) = (2, 1)$ or $(p, q) = (3, 2)$, depending on the term considered.

One can use this E -decomposition of \mathbf{J}' , Eq. (A9), combined with the scaling of the individual E -signals, Eq. (A10), to show by inspection that the terms neglected in Eq. (10), *i.e.* terms of the form $\frac{1}{V} \langle V^S J' \rangle$ and $\frac{1}{V} \langle J' J' \rangle$, are indeed negligible in the TD limit.

Appendix B: Equivalence between renormalization and decorrelation

Let us consider only isotropic systems, such as $h_{\alpha\beta}^S \equiv h^S \delta_{\alpha\beta}$. In this section we use different brackets $\langle \cdot \rangle$ and $\langle \cdot \rangle_{\text{can}}$ to indicate an equilibrium average in the microcanonical and the canonical ensemble, respectively. From the explicit form of the canonical Boltzmann distribution:

$$P_{\text{can}}(\{\mathbf{r}, \mathbf{v}\}) \sim \exp \left[-\frac{U(\{\mathbf{r}\})}{k_B T} \right] \prod_i \exp \left[-\frac{m_i v_i^2}{2k_B T} \right], \quad (\text{B1})$$

one can explicitly verify that each renormalized velocity $\mathbf{v}'_i = \mathbf{v}_i - \mathbf{W}^{S(i)}$ is independent of \mathbf{V}^S , for any species S . For example, given the linearity of the transformation and the Gaussian velocity distribution, it is sufficient to check that $\langle \mathbf{v}'_i \cdot \mathbf{V}^S \rangle_{\text{can}} = 0$. As a consequence $\langle \mathbf{J}_{\text{ren}} \cdot \mathbf{V}^S \rangle_{\text{can}} = 0$, the current \mathbf{J}_{ren} being sum of functions of \mathbf{v}'_i and therefore uncorrelated with \mathbf{V}^S . This result holds exactly for every finite number of particles and not only in the TD limit.

The standard formula relating the expectation values of fluctuations in different ensembles^{35–37} now reads:

$$\langle \mathbf{J}_{\text{ren}} \cdot \mathbf{V}^S \rangle = \sum_{\alpha,\beta} \frac{\partial(\beta w_\alpha)}{\partial M_\beta} \left(\frac{\partial \langle \mathbf{J}_{\text{ren}} \rangle_{\text{can}}}{\partial(\beta w_\alpha)} \frac{\partial \langle \mathbf{V}^S \rangle_{\text{can}}}{\partial(\beta w_\beta)} \right) + \quad (\text{B2})$$

$$+ \frac{\partial \beta}{\partial E} \left(\frac{\partial \langle \mathbf{J}_{\text{ren}} \rangle_{\text{can}}}{\partial \beta} \frac{\partial \langle \mathbf{V}^S \rangle_{\text{can}}}{\partial \beta} \right) + \mathcal{O}(N), \quad (\text{B3})$$

where E and \mathbf{M} are the total energy and momentum, whose conjugate quantities are β and $\beta \mathbf{w}$, \mathbf{w} being the mean centre of mass velocity. The renormalized current has a zero expectation value for every temperature and is by construction independent of any global drift of the system. Therefore all derivatives of \mathbf{J}_{ren} are zero and $\langle \mathbf{J}_{\text{ren}} \cdot \mathbf{V}^S \rangle \sim \mathcal{O}(N)$. Let us exploit this result and calculate the scalar product of \mathbf{J}_{ren} and a generic $\mathbf{V}^{S'}$. Using Eq. (9), in the TD limit one finds the following formal set of relations satisfied by h^S :

$$\left\langle \left(\mathbf{J}_{\text{bare}} - \sum_S h^S \mathbf{V}^S \right) \cdot \mathbf{V}^{S'} \right\rangle = 0, \quad \forall S', \quad (\text{B4})$$

which is exactly the same linear system used for the decorrelation technique. As discussed in the text, this implies the equivalence, in the TD limit, between the decorrelation and renormalization techniques.

Appendix C: Numerical check of theoretical thermodynamic scalings

We can numerically check the TD scaling of $\Delta \mathbf{J} = \mathbf{J}_{\text{bare}} - \mathbf{J}_{\text{ren}}$ predicted by Eq. (10), for the classical water model presented in the section III. We focus our attention

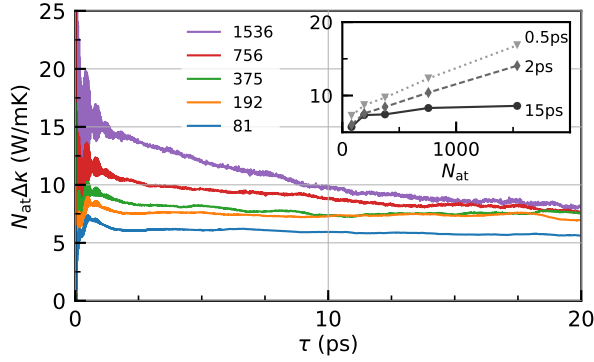


FIG. 4. Behavior of $N_{\text{at}}\Delta\kappa(\tau)$, defined in Eq. (C1), for a flexible water model at 300 K. Each curve refers to a different number of particles N_{at} , reported in the legend. Inset: $N_{\text{at}}\Delta\kappa(\tau)$ at fixed τ , as a function of N_{at} . At short times the magnitude grows with N_{at} , since $\Delta\kappa(\tau)$ tends to a finite limit; instead, the converged value for large τ remains stable and compatible with a $\mathcal{O}(1/N_{\text{at}})$ decay of $\Delta\kappa(\tau)$.

on the TD scaling for large number of atoms N_{at} of the function:

$$N_{\text{at}}\Delta\kappa(\tau) = \frac{N_{\text{at}}}{3Vk_B T^2} \int_0^\tau \langle \Delta\mathbf{J}(t)\Delta\mathbf{J}(0) \rangle dt, \quad (\text{C1})$$

plotted in Fig. 4. From the arguments presented in section III, two different TD scaling regimes are expected and observed as a function of τ : at short times $\Delta\kappa(\tau)$ tends to a finite value (in the TD limit) given by Eq. (10), thus $N_{\text{at}}\Delta\kappa(\tau)$ diverges linearly with N_{at} ; at long time lags the contribution given by Eq. (10) integrates to zero and we observe that $N_{\text{at}}\Delta\kappa(\tau)$ tends to a finite limit, hence $\Delta\kappa(\tau) \sim \mathcal{O}(1/N_{\text{at}})$.

Appendix D: Computational details

a. Classical Water - Simulation details Classical simulations of water have been performed using LAMMPS²⁵, considering a flexible model of water²⁶, in a cubic box with an edge of 18.6 Å containing 216 molecules, obtaining the experimental density. The integration time step was 0.5 fs. The system was thermalized in the NVT ensemble at 300 K for 200 ps using the stochastic velocity rescaling thermostat³⁸ with a coupling time of 200 fs, followed by 50 ps of equilibration in the NVE ensemble. Subsequently, the system has been evolved in the NVE ensemble for 10 ns, and the heat flux has been computed every 1 fs using the classical definition, Eq. (D4).

b. Silica - Simulation details The classical trajectory of a-SiO₂ has been generated using LAMMPS²⁵ and the BKS force field²⁷. A previously generated 72-atom sample of a-SiO₂ was considered, in a cubic box with an edge of 20.3 Å. The integration time step was 1.0 fs. The system was thermalized in the NVT ensemble at 300 K for 500 ps, followed by 100 ps of equilibration in the NVE

ensemble. Subsequently, the system has been evolved in the NVE ensemble for 1 ns, while the heat flux was computed every 1 fs using the classical definition, Eq. (D4). 100 ps of this trajectory were used for the *ab initio* calculation of the heat flux. To estimate the thermal conductivity, we used cepstral analysis¹⁶ with $f^* \approx 17$ THz. We verified that the value of κ does not vary with respect to this choice.

c. Ab initio Water - Simulation details The simulation setting is the same as Ref. 1. The trajectory length analysed was 90 ps. The parameters used in cepstral analysis are $f^* \approx 9$ THz, and in this case the P^* value was multiplied by a factor 1.5 to reduce any bias possibly due to the fast variation of the spectrum at frequency close to zero.

d. Green-Kubo integral The simplest way to estimate the thermal conductivity κ consists in a direct calculation of the GK equation (1) as a function of the upper limit of integration. We have that $\kappa = \lim_{\tau \rightarrow \infty} \kappa(\tau)$, where $\kappa(\tau) = \frac{1}{3Vk_B T^2} \int_0^\tau \langle \mathbf{J}(t) \cdot \mathbf{J}(0) \rangle dt$. The autocorrelation function $\langle \mathbf{J}(t) \cdot \mathbf{J}(0) \rangle$ can be evaluated numerically from a discretized-time series as an average over many time origins:³⁹

$$\langle \mathbf{J}(t) \cdot \mathbf{J}(0) \rangle = \frac{1}{t_{\text{max}}} \sum_{\alpha=1}^3 \sum_{t_0=0}^{t_{\text{max}}} J^\alpha(t_0+t) J^\alpha(t_0), \quad (\text{D1})$$

where $\alpha = 1, 2, 3$ indicate the cartesian components, and we assume $t_{\text{max}} + t \leq t_{\text{run}}$. An estimate of the statistical error of Eq. (D1) and of the estimator $\kappa(\tau)$ can be obtained by block analysis,^{39,40} however the convergence value of $\kappa(\tau)$ for $\tau \rightarrow \infty$ is generally difficult to identify and more advanced techniques such as cepstral analysis are needed.

e. Classical heat flux In a system of N atoms interacting through a classical force field $U(\mathbf{r}_1, \mathbf{r}_2, \dots, \mathbf{r}_N)$ the “standard” definition of the energy density is written in terms of local atomic energies as:

$$\epsilon(\mathbf{r}, \Gamma_t) = \sum_i \delta(\mathbf{r} - \mathbf{r}_i) \epsilon_i(\Gamma_t), \quad (\text{D2})$$

$$\epsilon_i(\Gamma_t) = \frac{1}{2} m_i v_i^2 + U_i(\{\mathbf{r}\}) + \bar{\epsilon}^{S(i)}, \quad (\text{D3})$$

where U_i are atomic potential energies whose sum is the total potential energy of the system, and $\bar{\epsilon}^{S(i)}$ is a species-dependent formation energy that is usually set to zero. The energy flux can be written as:

$$\mathbf{J}(t) = \sum_i \mathbf{v}_i \epsilon_i + \sum_{i,j} (\mathbf{r}_i - \mathbf{r}_j) \mathbf{f}_{ij} \cdot \mathbf{v}_i, \quad (\text{D4})$$

where $\mathbf{f}_{ij} = -\frac{\partial U_j}{\partial \mathbf{r}_i}$ is the contribution of the j -th atom to the force acting on the i -th atom, $\sum_j \mathbf{f}_{ij} = \mathbf{f}_i$, and $\mathbf{f}_{ij} = -\mathbf{f}_{ji}$. In the case of two-body potentials, such as the ones considered in this paper, the common choice consists in splitting the potential energy evenly between the two interacting atoms, that is: $U_j = \frac{1}{2} \sum_i U(\mathbf{r}_i -$

\mathbf{r}_j) and $\mathbf{f}_{ij} = -\frac{1}{2}\nabla_{\mathbf{r}_i}U(\mathbf{r}_i - \mathbf{r}_j)$. This is of course an arbitrary choice: the gauge invariance principle ensures that any other choice such that $\sum_i U_i = U$ leads to the same thermal conductivity.²

For two-body force fields, Eq. (D4) is implemented in LAMMPS and can be computed using the `compute heat/flux` command.

f. First-principles heat flux We report here for completeness the formulas used for the evaluation of the first-principles (DFT) heat flux. The bare current is given by the sum of the following components:

$$\mathbf{J}_{KS} = \sum_v \left(\langle \varphi_v | \mathbf{r} \hat{H}_{KS} | \dot{\varphi}_v \rangle + \varepsilon_v \langle \dot{\varphi}_v | \mathbf{r} | \varphi_v \rangle \right), \quad (\text{D5})$$

$$\mathbf{J}_H = \frac{1}{4\pi} \int \dot{u}_H(\mathbf{r}) \nabla u_H(\mathbf{r}) d\mathbf{r}, \quad (\text{D6})$$

$$\mathbf{J}'_0 = \sum_i \sum_v \langle \varphi_v | (\mathbf{r} - \mathbf{r}_i) (\mathbf{v}_i \cdot \nabla_{\mathbf{r}_i} \hat{v}_0) | \varphi_v \rangle, \quad (\text{D7})$$

$$\mathbf{J}_0 = \sum_i \left[\mathbf{v}_i e_i^0 + \sum_{j \neq i} (\mathbf{r}_i - \mathbf{r}_j) (\mathbf{v}_j \cdot \nabla_{\mathbf{r}_j} w_i) \right], \quad (\text{D8})$$

$$\mathbf{J}_{XC} = \begin{cases} 0 & (\text{LDA}) \\ -\int \rho(\mathbf{r}) \dot{\rho}(\mathbf{r}) \partial \epsilon_{GGA}(\mathbf{r}) d\mathbf{r} & (\text{GGA}), \end{cases} \quad (\text{D9})$$

where \mathbf{r}_i and \mathbf{v}_i are the positions and velocities of the i -atom. The electronic degrees of freedom are described by the wavefunctions φ_v . The electron charge is assumed to be one and the remaining symbols are instead defined as:

- e_i^0 : ionic energy, equal to $\frac{1}{2}m_i v_i^2 + w_i$;
- ϵ_{XC} : local XC energy per particle, defined by the relation: $E_{XC} = \int \epsilon_{XC}[\rho](\mathbf{r}) \rho(\mathbf{r}) d\mathbf{r}$. “LDA” and “GGA” in Eq. (D9) indicate the local-density and generalized-gradient approximations to the XC energy functional ;
- ϵ_v : electronic eigenvalues ;
- \hat{H}_{KS} : instantaneous Kohn-Sham (KS) Hamiltonian ;
- m_i : atomic mass ;
- \mathbf{r} : multiplicative position operator ;
- $\rho(\mathbf{r})$: ground-state electron-density distribution ;
- u_H and u_{XC} : Hartree and exchange-correlation (XC) potentials ;
- \hat{u}_0 : ionic (pseudo-) potential acting on the electrons ;
- w_i : electrostatic energy, equal to $\frac{1}{2} \sum_{j \neq i} \frac{Z_i Z_j}{|\mathbf{r}_i - \mathbf{r}_j|}$;
- Z_i : atomic charge ;
- $\partial \epsilon_{GGA}$: derivative of the GGA XC local energy per particle with respect to density gradients ,

- ∇ : gradient with respect to the spatial coordinate \mathbf{r} ;
- $\nabla_{\mathbf{r}_i}$: gradient with respect to the atomic position \mathbf{r}_i ;
- $\langle \rangle$: standard scalar product between wavefunctions ;
- $\dot{}$: derivative with respect to time ;

More technical details on a possible implementation can be found in the references^{1,24}.

Finally, even if we reported the precise expressions used in this work, we note that the decorrelation and renormalization techniques are general and do not depend on the specific definition of the bare heat flux. As discussed in the main text, the decorrelated current is evaluated by solving the linear system of Eq. (6), and plugging in the resulting $\{\lambda_n\}$ coefficients into Eq. (2). The renormalized currents are instead evaluated using the same expression of the bare ones, but replacing velocities with their renormalized values.

Appendix E: Electronic current

The adiabatic electronic flux \mathbf{J}_{el} can be evaluated as:⁴¹

$$\mathbf{J}_{\text{el}} = 2\Re \sum_v \langle \varphi_v | \mathbf{r} | \dot{\varphi}_v \rangle, \quad (\text{E1})$$

following the same notation of Appendix D. This expression can be derived from the conservation equation for the electronic density ρ :

$$\nabla \cdot \mathbf{j}_{\text{el}}(\mathbf{r}, t) = -\dot{\rho}(\mathbf{r}, t), \quad (\text{E2})$$

where $\mathbf{j}_{\text{el}}(\mathbf{r})$ is the electronic current density. The flux is then defined as $\mathbf{J}_{\text{el}} = \int \mathbf{j}_{\text{el}}(\mathbf{r}) d\mathbf{r} \sim \int \dot{\rho}(\mathbf{r}, t) \mathbf{r} d\mathbf{r}$, where boundary terms can be neglected^{4,42}. Inserting in the last expression the definition of ρ in terms of the electronic wavefunctions, one obtains Eq. (E1), which is an expression well defined under periodic boundary conditions.²⁴ We note that the same current can be alternatively evaluated in terms of the Born-effective charges⁴².

The electronic current is the difference between the total charge current (defined as the atom’s Born charge times its velocity and summed over the atoms) and its ionic component (here defined considering the nucleus plus the valence electrons). Analogously to the particle current, in the electrically insulating systems considered in this work the electronic current \mathbf{J}_{el} is a non-diffusive signal (because the difference between the electronic and the particle current is itself a non-diffusive signal).^{1,3,4}

* ISR@zurich.ibm.com

† (Present address:) Theory and Simulation of Materials

- (THEOS), and National Centre for Computational Design and Discovery of Novel Materials (MARVEL), École Polytechnique Fédérale de Lausanne, CH-1015 Lausanne, Switzerland.
- ¹ A. Marcolongo, P. Umari, and S. Baroni, *Nature Phys.* **12**, 80 (2016).
 - ² L. Ercole, A. Marcolongo, P. Umari, and S. Baroni, *J. Low Temp. Phys.* **185**, 79 (2016).
 - ³ F. Grasselli and S. Baroni, *Nature Physics* **15**, 967 (2019).
 - ⁴ S. Baroni, R. Bertossa, L. Ercole, F. Grasselli, and A. Marcolongo, “Heat transport in insulators from ab initio greenkubo theory,” in *Handbook of Materials Modeling: Applications: Current and Emerging Materials*, edited by W. Andreoni and S. Yip (Springer International Publishing, Cham, 2018) pp. 1–36, 2nd ed., arXiv:1802.08006 [cond-mat.stat-mech].
 - ⁵ M. S. Green, *J. Chem. Phys.* **20**, 1281 (1952); *J. Chem. Phys.* **22**, 398 (1954).
 - ⁶ R. Kubo, *J. Phys. Soc. Jpn.* **12**, 570 (1957); R. Kubo, M. Yokota, and S. Nakajima, *J. Phys. Soc. Jpn.* **12**, 1203 (1957).
 - ⁷ J. Kang and L.-W. Wang, *Phys. Rev. B* **96**, 20302 (2017).
 - ⁸ N. J. English and J. S. Tse, *Computational Materials Science* **126**, 1 (2017); J. S. Tse, N. J. English, K. Yin, and T. Iitaka, *The Journal of Physical Chemistry C* **122**, 10682 (2018).
 - ⁹ E. Lampin, Q.-H. Nguyen, P. A. Francioso, and F. Cleri, *Applied Physics Letters* **100**, 131906 (2012).
 - ¹⁰ F. Müller-Plathe, *The Journal of Chemical Physics* **106**, 6082 (1997).
 - ¹¹ M. Puligheddu, F. Gygi, and G. Galli, *Phys. Rev. Materials* **1**, 060802 (2017).
 - ¹² S. Stackhouse, L. Stixrude, and B. B. Karki, *Physical review letters* **104**, 208501 (2010).
 - ¹³ C. Melis, S. Dettori, Riccardo adn Vandermeulen, and L. Colombo, *The European Physical Journal B* **87** (2014).
 - ¹⁴ M. Zhang, E. Lussetti, L. E. S. de Souza, and F. Müller-Plathe, *The Journal of Physical Chemistry B* **109**, 15060 (2005).
 - ¹⁵ L. Lindsay, A. Katre, A. Cepellotti, and N. Mingo, *Journal of Applied Physics* **126**, 050902 (2019).
 - ¹⁶ L. Ercole, A. Marcolongo, and S. Baroni, *Sci. Rep.* **7**, 15835 (2017).
 - ¹⁷ L. d. S. Oliveira and P. A. Greaney, *Phys. Rev. E* **95**, 023308 (2017).
 - ¹⁸ C. Carbogno, R. Ramprasad, and M. Scheffler, *Phys. Rev. Lett.* **118**, 175901 (2017).
 - ¹⁹ R. Bertossa, F. Grasselli, L. Ercole, and S. Baroni, *Phys. Rev. Lett.* **122**, 255901 (2019), arXiv:1808.03341.
 - ²⁰ M. Salanne, D. Marrocchelli, C. Merlet, N. Ohtori, and P. A. Madden, *Journal of Physics: Condensed Matter* **23**, 102101 (2011).
 - ²¹ K. Esfarjani, G. Chen, and H. T. Stokes, *Phys. Rev. B* **84**, 085204 (2011).
 - ²² S. Stackhouse and L. Stixrude, *Reviews in Mineralogy and Geochemistry* **71**, 253 (2010).
 - ²³ L. Ercole, *Ab Initio Simulation of Heat Transport in Silica Glass*, Ph.D. thesis, Scuola Internazionale Superiore di Studi Avanzati, Trieste (2018).
 - ²⁴ A. Marcolongo, *Theory and ab initio simulation of atomic heat transport*, Ph.D. thesis, Scuola Internazionale Superiore di Studi Avanzati, Trieste (2014).
 - ²⁵ S. Plimpton, *J. Comp. Phys.* **117**, 1 (1995).
 - ²⁶ J. Alejandro, G. A. Chapela, F. Bresme, and J. P. Hansen, *J. Chem. Phys.* **130** (2009), 10.1063/1.3124184.
 - ²⁷ B. W. H. van Beest, G. J. Kramer, and R. A. van Santen, *Phys. Rev. Lett.* **64**, 1955 (1990).
 - ²⁸ P. Giannozzi, O. Andreussi, T. Brumme, O. Bunau, M. B. Nardelli, M. Calandra, R. Car, C. Cavazzoni, D. Ceresoli, M. Cococcioni, N. Colonna, I. Carnimeo, A. D. Corso, S. de Gironcoli, P. Delugas, R. A. D. Jr, A. Ferretti, A. Floris, G. Fratesi, G. Fugallo, R. Gebauer, U. Gerstmann, F. Giustino, T. Gorni, J. Jia, M. Kawamura, H.-Y. Ko, A. Kokalj, E. Küçükbenli, M. Lazzeri, M. Marsili, N. Marzari, F. Mauri, N. L. Nguyen, H.-V. Nguyen, A. O. de-la Roza, L. Paulatto, S. Poncé, D. Rocca, R. Sabatini, B. Santra, M. Schlipf, A. P. Seitsonen, A. Smogunov, I. Timrov, T. Thonhauser, P. Umari, N. Vast, X. Wu, and S. Baroni, *Journal of Physics: Condensed Matter* **29**, 465901 (2017).
 - ²⁹ J. P. Perdew, K. Burke, and M. Ernzerhof, *Phys. Rev. Lett.* **77**, 3865 (1996).
 - ³⁰ D. R. Hamann, *Phys. Rev. B* **88**, 085117 (2013); M. Schlipf and F. Gygi, *Computer Physics Communications* **196**, 36 (2015).
 - ³¹ T. Yamane, N. Nagai, S.-i. Katayama, and M. Todoki, *Journal of Applied Physics* **91**, 9772 (2002); J. M. Larkin and A. J. H. McGaughey, *Phys. Rev. B* **89**, 144303 (2014); Y. Touloukian, R. Powell, C. Ho, and P. Klemens, *Thermophysical properties of matter - the TPRC data series. Volume 2. Thermal conductivity - nonmetallic solids. (Reannouncement). Data book* (IFI/Plenum, New York, 1970); D. G. Cahill, *Review of Scientific Instruments* **61**, 802 (1990).
 - ³² L. Ercole and R. Bertossa, “ThermoCepstrum: a code to estimate transport coefficients from the cepstral analysis of a multi-variate current stationary time series,” <https://github.com/lorisercole/thermocepstrum> (2017–2018).
 - ³³ Since \mathbf{V}^{Si} and \mathbf{V}^{O} are trivially proportional, due to the conservation of total momentum, the decorrelation of a current with respect to one or the other yields the same results.
 - ³⁴ H. B. G. Casimir, *Reviews of Modern Physics* **17**, 343 (1945).
 - ³⁵ J. L. Lebowitz, J. K. Percus, and L. Verlet, *Phys. Rev.* **153**, 250 (1967).
 - ³⁶ D. C. Wallace, *Statistical Physics of Crystals and Liquids* (WORLD SCIENTIFIC, 2003).
 - ³⁷ A. Marcolongo and N. Marzari, *Phys. Rev. Materials* **1**, 025402 (2017).
 - ³⁸ G. Bussi, D. Donadio, and M. Parrinello, *The Journal of Chemical Physics* **126**, 014101 (2007).
 - ³⁹ M. P. Allen and D. J. Tildesley, *Computer Simulation of Liquids* (Clarendon Press, 1989).
 - ⁴⁰ D. Frenkel and B. Smit, *Understanding Molecular Simulation: From Algorithms to Applications*, second edition ed. (Academic Press, 2002).
 - ⁴¹ D. J. Thouless, *Phys. Rev. B* **27**, 6083 (1983).
 - ⁴² T. Sun and R. Wentzcovitch, *Chemical Physics Letters* **554**, 15 (2012).